

Limit Analyses of the Active Earth Pressure on Rigid Retaining Walls under Strip Loading on Backfills



N. Tallah^{1*}, A. Boulaouad², A. Bouaicha³

¹ Laboratoire de Développement des Géomatériaux, University of M'sila, M'sila 28000, Algeria

² Department of Civil Engineering, Faculty of Technology, University Med Boudiaf of M'sila, M'sila 28 000, Algeria

³ Civil Engineering Research Laboratory, University of Biskra, BP 145 RP, Biskra 07000, Algeria

Corresponding Author Email: naoui.tallah@univ-msila.dz

<https://doi.org/10.18280/acsm.460104>

ABSTRACT

Received: 11 February 2022

Accepted: 26 February 2022

Keywords:

active earth pressure, failure mechanism, limit analysis, retaining wall, strip load

Recent studies of retaining walls include experimental studies, numerical analysis and analytical models. Although active earth pressure against retaining structures has received much attention, the evaluation of active earth pressure of backfill when loaded by a strip foundation, has been slightly studied. This paper studies the effect of a strip load on the active pressure force and the distribution of the horizontal stresses on a rigid wall, using a finite element limit analysis. The strip loading is located at different distances from the vertical face of the wall. The OptumG2 code is used to analyze the effect of width of strip surcharge (soil-wall), interface friction angle and soil internal friction angle. New interesting results are demonstrated and presented here: the dependency of the active earth pressure coefficient on both position and width of the strip load, in one hand, and the effect of the internal friction angle of the soil, the soil-wall interface, and the position of the strip loading on the failure mechanism, in the other hand.

1. INTRODUCTION

Active earth pressure is a significant problem in geotechnical engineering, because it causes instability in structures such as retaining walls. Active earth pressure can be evaluated by applying the classical Coulomb's [1] and Rankine's [2] theories. Upper and lower bound limit analysis methods are also used to solve the earth pressure. Kumar and Chitikela [3] and Santhoshkumar and Ghosh [4] solved the earth pressure using the method of stress characteristics. Muraro et al. [5], Chowdhury [6] and Veiskarami et al. [7] performed finite element method to analyze the active earth pressure. The finite element method seems to be the most suitable method for studying support problems. It allows modeling the behavior of all the elements involved in the behavior of the structure (soil, wall, water, surcharge, etc.) as well as the different couplings between these elements. However, many developments are still necessary on both implementation of the method (whose inputs and outputs should be simplified) and modeling of soil behavior.

In many earth retaining problems, it is necessary to consider additional earth pressures produced by surcharge strip loads acting on the soil surface behind the wall. The problem of surcharge on retaining wall is a common problem, particularly for supports in urban or maritime sites due to the presence of surrounding constructions. From a theoretical point of view, two methods with divergent assumptions allow to take into account the effect of a surcharge, elastic methods and methods based on limit equilibrium. Historically, Coulomb [1] was the first to think about the presence of a surcharge on the supported median which considers the equilibrium at failure of the system composed of the structure and the surcharge.

One can also distinguish the specific methods which consist in determining the influence of the surcharge on the wall independently of the earth. Then, the principle of superposition stated by Caquot allows determining the global action of the earth and the surcharge on the wall, by simple addition of the effects [8, 9]. These methods are well suited to the calculation of the influence of an infinite uniform surcharge. In the case of other types of surcharges, it is necessary to make some assumptions about the distribution of pressures behind the wall.

The choice of an elastic or plastic soil model is fundamental for modeling the transmission of the surcharge. However, none of the methods can claim to deal with all surcharge cases, nor the entire behavior of the structure, from the start of loading to its eventual failure.

The modeling of the interaction between the wall and the foundation from the Mohr-Coulomb model did not give satisfactory results and the development of numerical modeling for the study of retaining structures can only go through the optimization of the programming of advanced constitutive laws and increased accessibility to the determination of their parameters [10].

Two approximate methods for calculating the strip load-generated lateral force have also been proposed by Blum [11]. The earth pressure distributions obtained with these methods differ significantly from each other and may lead to either very conservative or unsafe solutions. Jarquio [12] and Misra [13] provided solutions for lateral stresses on the wall due to the strip load based on Boussinesq's elastic half space solution. Steenfelt and Hansen [14], Motta [15] and Greco [16] extended Coulomb approach, in which the evaluation of active earth force when a strip load act is obtained by limit

equilibrium method.

Jarquio [12] concludes that Boussinesq’s elastic-based solution for lateral stresses on a completely rigid wall is a general solution applicable to both yielding and unyielding retaining wall structures. But, Steenfelt and Hansen [14] recommend Boussinesq’s solution only for unyielding structures, and that for the active state retaining walls the coulomb approach would be more reasonable.

In the present study, a series of numerical computations using the two-dimensional (2-D) FE limit analysis code OptumG2 [17] is carried out in order to examine the effect of a partial surcharge on the active pressure force and the distribution of horizontal stresses on the wall; this surcharge is located at different positions of a horizontal profile backfill behind a vertical retaining wall. The approach used in this paper is based on upper bound theorem of limit analysis method and can be used to determine active lateral force due to simultaneous effect of both soil weight and surcharge of strip load.

The results of the present analysis show that the effect of a strip load on the active pressure and on the active pressure coefficient depends on the position of the load, the width of the surcharge and the angle of internal friction of the soil; for the failure mechanism, it can be seen that the failure plane depends on the angle of internal friction of the soil and on the ratio a/H and that the angle of friction between the backfill and the wall δ has no influence on the plane shape of the rupture.

The remainder of this paper is organized as follows. In section 2 the previous studies are summarized. In Section 3 it is the description of the problem. In Section 4 the numerical model is validated with those of the methods which are currently used in the determination of strip load. In Section 5 we the obtained results are discussed and the Section 6 concludes the work.

2. LITERATURE REVIEW

There are very few available literatures showing the influence of external surcharge load on retaining walls, which is a common practice [14, 15, 18-21]. Steenfelt and Hansen [14] provided complete analytical solution to demonstrate the effect of strip load on the design of sheet pile walls using Brinch Hansen’s earth pressure theory, and suggest that the elastic solution applies only to unyielding structures, and that for structures in the active state of failure a Coulomb analysis would be more appropriate. Motta [15] provided a closed form solution for retaining wall having inclined backfill with surcharge at different distances. Georgiadis and Anagnostopoulos [18] conducted the model sheet pile wall tests in sand to investigate the effect of surcharge strip loads on wall behavior. Graphical solutions, combining both elastic and plastic approaches, have been used to determine lateral earth pressure due to external surcharge load.

Farzaneh et al [22] proposed a solution to active earth pressure on rigid walls caused by strip loads via the upper-bound limit analysis method. Greco [16] calculated active earth thrust of backfill on a retaining wall subjected to a strip load using a hybrid approach. Hou and Shu [23] provided a trial wedge approach to lateral earth pressure on rigid walls using the limit equilibrium method.

Most of the previous studies focus on the active pressure force and neglect the calculation of the active pressure coefficient, whereas in this study importance is given to the

calculation of the active pressure coefficient and is presented in the form of dimensionless design charts relating the mechanical characteristics of the soil, strip load conditions and active earth pressure.

3. PROBLEM DESCRIPTION

The problem of the current study considers a rigid retaining wall having a height $H=10$ m (very high), the geometry and finite element mesh are shown in Figure 1.

Dead weights were placed some distance a behind the wall imposing a surcharge of strip load, q , the position from the wall of the strip surcharge varies from $a/H=0$ to $a/H=1$ with 0.1 increments (Figure 2). The value of strip surcharge is fixed at $q=200$ kN/m² and b , which is the width of the strip load, is fixed at $b/H=0.2$ and $b/H=0.3$.

An elastoplastic constitutive model is used to represent the stress–strain behavior of soil, obeying Mohr–Coulomb failure criteria with the associative flow rule. The elastic properties are young’s modulus $E=35$ MPa, and Poisson’s ratio $\nu=0.3$. The cohesion $c=0$ and the angle of internal friction ϕ is varied from 30° to 40° in 5° increments. Of the flow rule, it is considered only the non-associative case where the dilation angle $\psi=0$. The magnitude of soil weight is supposed equal to $\gamma=20$ kN/m³. A linearly elastic model is used to simulate the concrete retaining wall. The interface elements are used to model the soil–structure interaction. The parameters of interface have the following values: a friction angle $\delta=0, 1^\circ, \phi/3$ and $2\phi/3$.

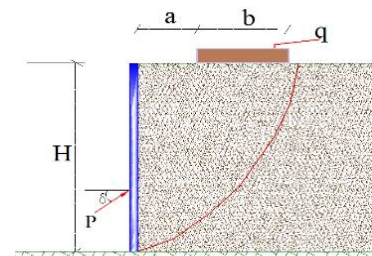


Figure 1. Geometry of a retaining wall– soil system

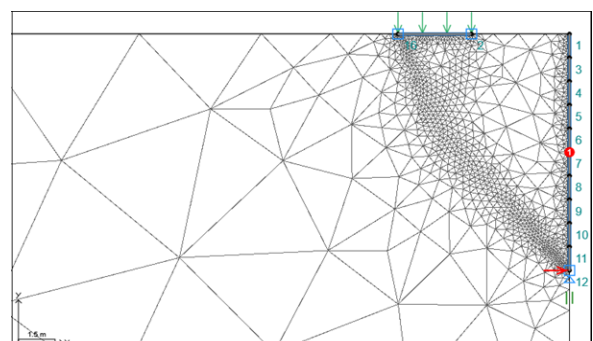


Figure 2. Finite mesh for a retaining wall for $a/H=0.3$

4. MODEL VALIDATION

In order to validate the numerical modeling procedure, the results obtained were compared with those of the methods which are currently used in the determination of strip load generated lateral earth pressures as the conventional Coulomb earth pressure analysis [14, 15], the lateral earth forces due to

soil weight and strip load were obtained using the wedge equilibrium analysis. This approach shown in Figure 3 is, in fact, an extension of the conventional Coulomb active earth pressure analysis, and a method proposed by Ghanbari and Taheri [24].

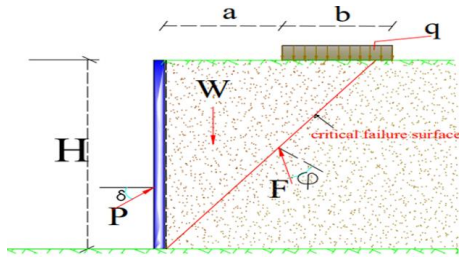


Figure 3. Limit equilibrium method

To mobilize the lateral pressure force up to rupture, in the boundary conditions, one leaves free displacement in the horizontal direction and applies a lateral force incrementally until rupture; Chauhan VB, Dasaka SM [25], to mobilize the lateral pressure behind the wall with relief shelves has to apply a continuous load in increments until failure, this approach remains valid in the case where the uniformly distributed load is continuous, if the load is partial this approach will be valid in the case of load-bearing capacity study.

Figure 4 provides comparison between methods. In this Figure, ratio $P/b \cdot q$ obtained for different distances of the strip load from the wall (a/H) is shown. In both analyses, lateral earth force decreases significantly as the strip load distance increases. The results of the present method are higher (better) than those of limit equilibrium method. This improvement when $a/H=0.4$, attains 5% and 10% for $q/\gamma H=1$ and $q/\gamma H=2$, respectively.

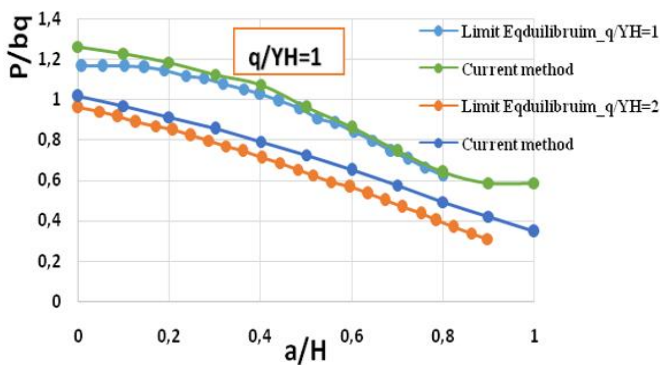


Figure 4. Comparison of current method with extended Coulomb approach for: $\phi=35^\circ$, $b/H=0.2$, $\delta/\phi=1/2$

Table 1. A comparison for lateral force induced by a linear load between current method values and those proposed by Motta [15] and Ghanbari and Taheri [24]: $\phi=30^\circ$, $\gamma=20$ kN/m^3 , $\delta=10^\circ$, $H=10\text{m}$, $c=0$ kPa

q(kN/m)	d(m)	Active earth force (kN/m)		
		Current Method	Motta	Ghanbari and Taheri
20	2	313	324	322
	4	315	319	315
50	2	333	347	344
	4	337	335	322
100	2	380	359	380
	4	378	362	335

As it can be seen in Table 1, there is a good agreement between analyses. In addition, solution proposed by Ghanbari and Taheri [24] gives higher values when $d=2$ m (d = distance of linear load from the wall) in relation to the two other methods, whereas for $d=4$ m, current method and Motta's approach present higher values compared to Ghanbari and Taheri's solution. However, the maximum difference between present method and the two other methods is about 12%.

5. RESULTS AND DISCUSSION

This part summarizes and discusses the main results of the work carried out within the framework of this study. From the numerical simulations, we have drawn the graphs for the active coefficient pressure K_{aq} of the surcharge q , in the different situations corresponding to: a/H varying from 0 to 1 with a 0.2 increment, the surcharge intensity $q/\gamma H=1$, $b/H=0.2$ and 0.3, the internal friction angle Φ of the sand varying from 30° to 40° with a 5° increment and the angle of friction between the wall and the backfill having the two values: $\delta=\Phi/3$ and $\delta=2\Phi/3$.

5.1 Active earth pressure distribution

(a) $q/\gamma H=1$, $b/H=0.2$

In the case where the angle $\Phi = 30^\circ$ (Figures 5 and 6), one can notice the following about the curve describing the variation of the lateral pressure:

-It is almost linear for the values of the ratio $a/H=0, 0.2$ and 0.4 .

-From $a/H=0.6$ to $a/H=1$, it has two distinct parts: one increasing with a certain slope until the ratio $z/H=-0.3$, the second also increasing but with a smaller slope.

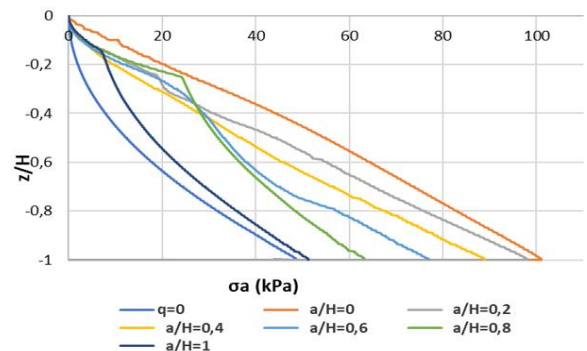


Figure 5. Active pressure for: $q/\gamma H=1$, $b/H=0.2$, $\Phi=30^\circ$, $\delta=\Phi/3$

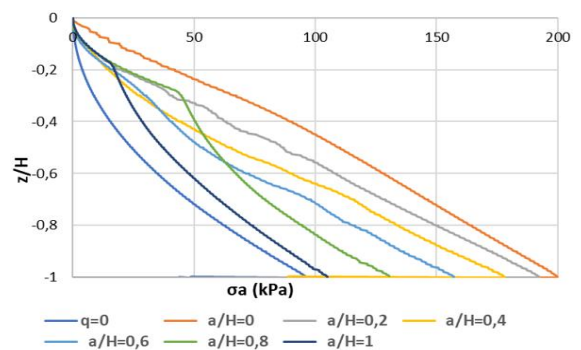


Figure 6. Active pressure for: $q/\gamma H=1$, $b/H=0.2$, $\Phi=30^\circ$, $\delta=2\Phi/3$

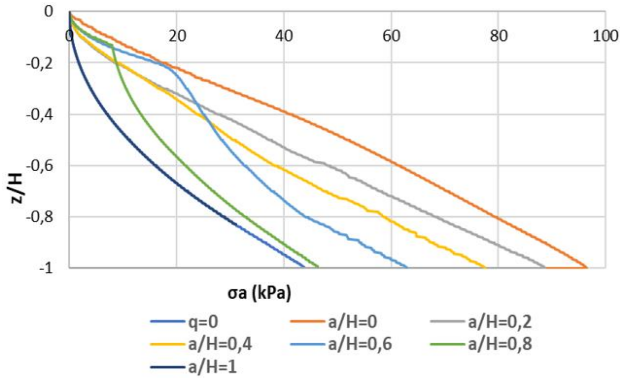


Figure 7. Active pressure, $q/\gamma H=1$, $b/H=0.2$, $\Phi=35^\circ$, $\delta=\Phi/3$

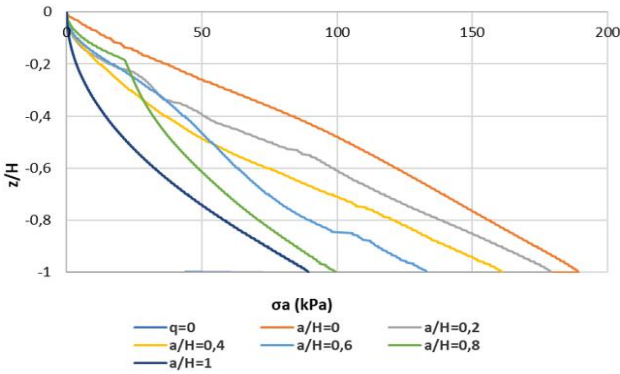


Figure 8. Active pressure, $q/\gamma H=1$, $b/H=0.2$, $\Phi=35^\circ$, $\delta=2\Phi/3$

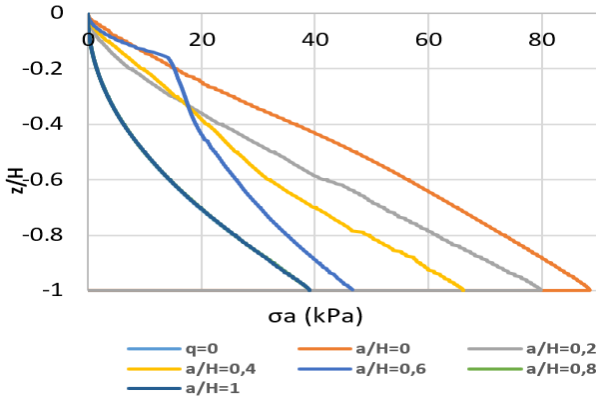


Figure 9. Active pressure, $q/\gamma H=1$, $b/H=0.2$, $\Phi=35^\circ$, $\delta=\Phi/3$

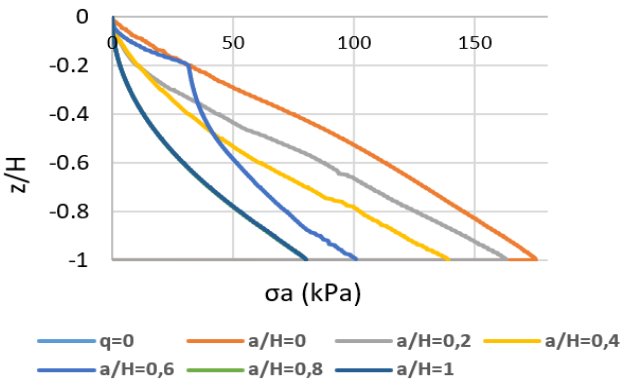


Figure 10. Active pressure, $q/\gamma H=1$, $b/H=0.2$, $\Phi=35^\circ$, $\delta=2\Phi/3$

If the angle $\Phi=35^\circ$, (Figures 7 and 8); from $a/H=0.6$, we distinguish two parts: one increasing until the ratio $z/H=-0.2$,

and the surcharge effect becomes zero for $a/H=1$. Where the angle $\Phi=40^\circ$ (Figures 9 and 10); from $a/H=0.6$, we distinguish two parts: one increasing until the ratio $z/H=0.16$, and the surcharge effect becomes zero from $a/H=0.8$.

(b) $q/\gamma H=1$, $b/H=0.3$

For the angle $\Phi=30^\circ$ (Figures 11 and 12), one can notice the following about the curve describing the variation of the lateral pressure:

-It is almost linear for the values of the ratio $a/H=0, 0.2, 0.4$ and 0.6 .

-For $a/H=0.6$ and $a/H=1$, it has two distinct parts: one increasing with a certain slope until the ratio $z/H=-0.3$, the second also increasing but with a smaller slope. In addition, the effect of the surcharge becomes zero from $a/H=0.1$. Where the angle $\Phi=35^\circ$, (Figures 13 and 14), for $a/H=0.6$, the curve is increasing until $z/H=-0.2$ and the effect of the surcharge becomes zero from $a/H=0.8$.

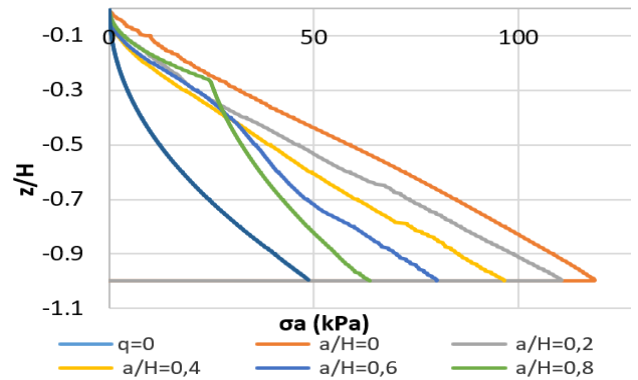


Figure 11. Active pressure, $q/\gamma H=2$, $b/H=0.2$, $\Phi=30^\circ$, $\delta=\Phi/3$

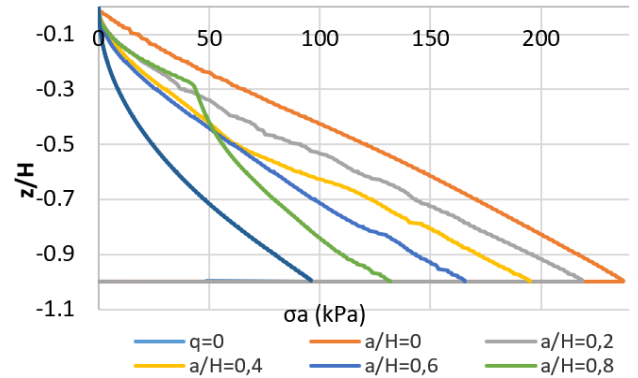


Figure 12. Active pressure, $q/\gamma H=2$, $b/H=0.2$, $\Phi=30^\circ$, $\delta=2\Phi/3$

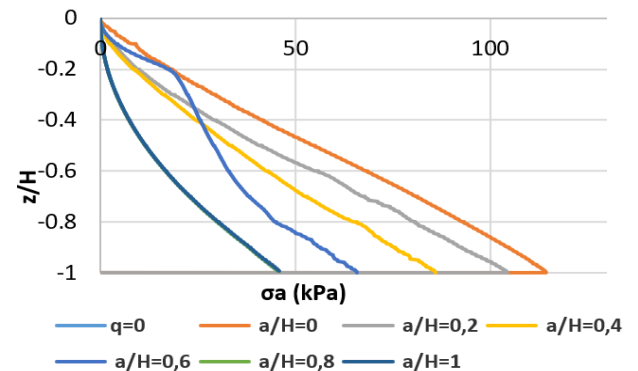


Figure 13. Active pressure, $q/\gamma H=2$, $b/H=0.2$, $\Phi=35^\circ$, $\delta=\Phi/3$

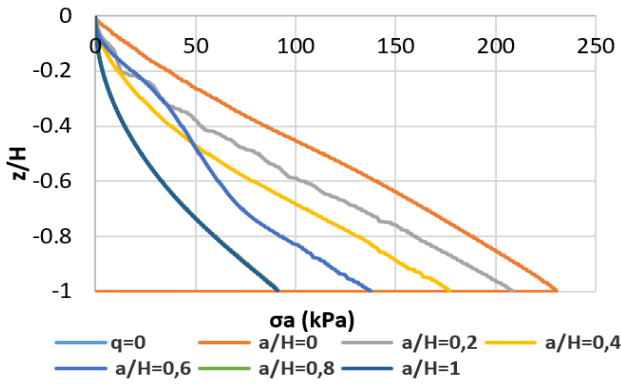


Figure 14. Active pressure, $q/\gamma H=2$, $b/H=0.2$, $\Phi=35^\circ$, $\delta=2\Phi/3$

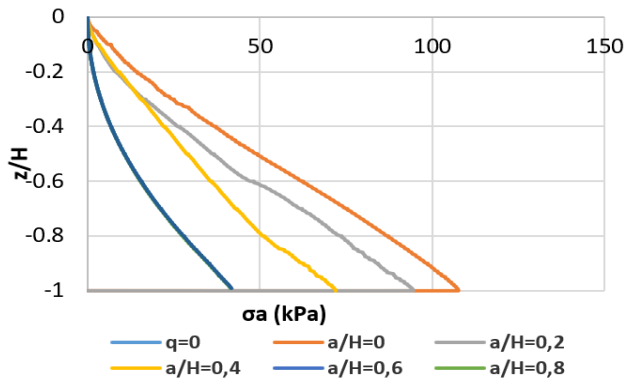


Figure 15. Active pressure, $q/\gamma H=2$, $b/H=0.2$, $\Phi=40^\circ$, $\delta=\Phi/3$

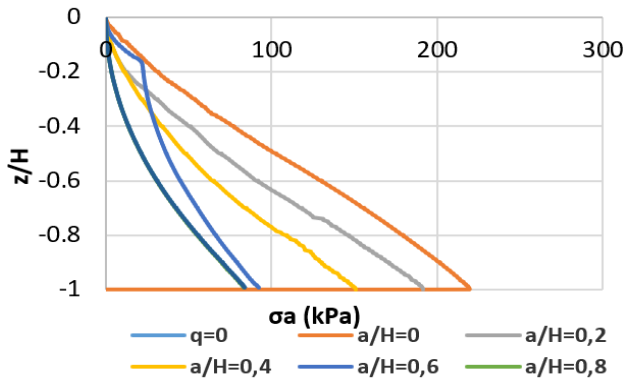


Figure 16. Active pressure, $q/\gamma H=2$, $b/H=0.2$, $\Phi=40^\circ$, $\delta=2\Phi/3$

In the case where the angle $\Phi=40^\circ$, (Figures 15 and 16), we notice that the effect of the surcharge becomes zero from $a/H=0.6$.

5.2 Active earth coefficient

To determine the active coefficient pressure K_{aq} of the surcharge, we apply the superposition method cited in the limit equilibrium method or coulomb analysis, this method has been recognized to be reliable for the case of the active state; derived solutions do not differ significantly with those derived from an upper-bound-limit analysis or from the method of characteristics. Furthermore, the Coulomb method allows solving earth-pressure problems with various boundary conditions so it seems appropriate to apply it in this note.

To determine the lateral earth pressure P_h produced by a

uniform surcharge load, the active earth pressure σ_a (due to the soil weight) is subtracted from the total active earth pressure σ_t (due to soil and surcharge). This latter is derived from a wedge equilibrium analysis (Figure 17) which provides the variation of the maximum lateral force P_h with depth z . Numerical differentiation of P_h with depth gives the total lateral pressure σ_T which is then used to calculate σ_{th} .

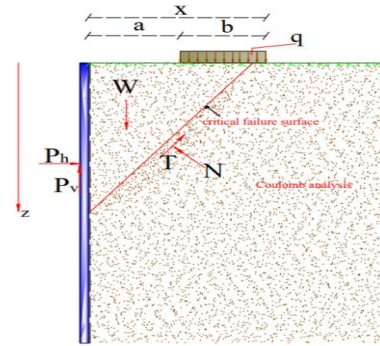


Figure 17. Coulomb analysis

$$\sigma = \sigma_{a(\text{earth})} + \sigma_{q(\text{surcharge})} = \sigma_{a(\text{earth})} + q \cdot K_{aq}$$

$$K_{aq} = \frac{\sigma - \sigma_{a(\text{earth})}}{q}$$

$P_{a(\text{earth})}$ is calculated in the case $q=0$.

(a) $q/\gamma H=1$, $b/H=0.2$

One can notice (see Figures 18 and 19) that the value of the active pressure coefficient K_{aq} increases at the start up to a limit value, this value varies with the variation of the a/H ratio, then stabilizes, and its value is maximum in the case where the position of the surcharge $a/H=0$, for the angle of internal friction $\Phi=30^\circ$, $K_{aq}=0.26$ if $\delta=\Phi/3$ and $K_{aq}=0.51$ for $\delta=2\Phi/3$.

From where the ratio $a/H=0.8$, one notice that there are two parts: an increasing linear part up to a limit value of the less important z/H ratio, and a second decreasing linear phase, and the maximum value $K_{aq}=0.1$ if $\delta=\Phi/3$ and $K_{aq}=0.18$ in the case $\delta=2\Phi/3$.

In the case where the angle $\Phi=35^\circ$, we notice the same variation of the active coefficient pressure K_{aq} as that of the angle $\Phi=30^\circ$, and the linear part becomes less important. From where the ratio $a/H=0.6$ we also notice that there are two parts, a linear part increasing up to a limit value of the ratio z/H less important, and a second decreasing linear phase, and the maximum value $K_{aq}=0.08$ if $\delta=\Phi/3$ and $K_{aq}=0.11$ for $\delta=2\Phi/3$, and from $a/H=1$ the value of K_{aq} takes the value $K_{aq}=0$, (see Figures 20 and 21).

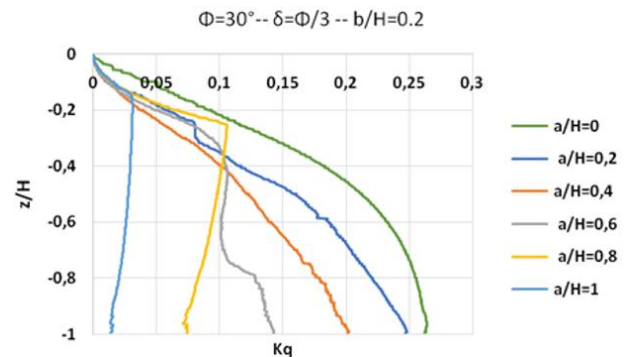


Figure 18. Pressure coefficient K_{aq} , $q/\gamma H=1$, $b/H=0.2$, $\Phi=30^\circ$, $\delta=\Phi/3$

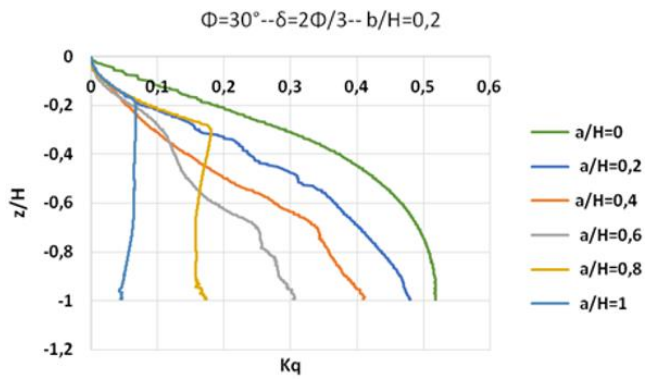


Figure 19. Pressure coefficient K_{aq} , $q/\gamma H=1$, $b/H=0.2$, $\Phi=30^\circ$, $\delta=2\Phi/3$

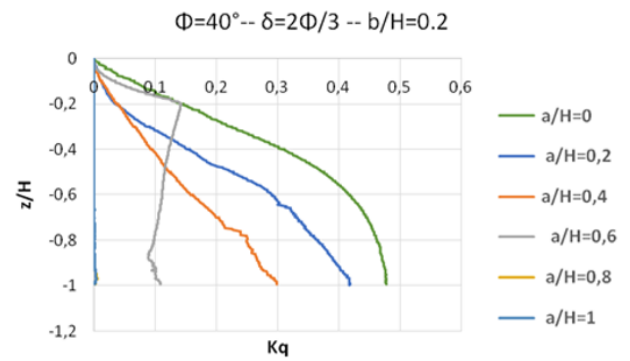


Figure 23. Pressure coefficient K_{aq} , $q/\gamma H=1$, $b/H=0.2$, $\Phi=40^\circ$, $\delta=2\Phi/3$

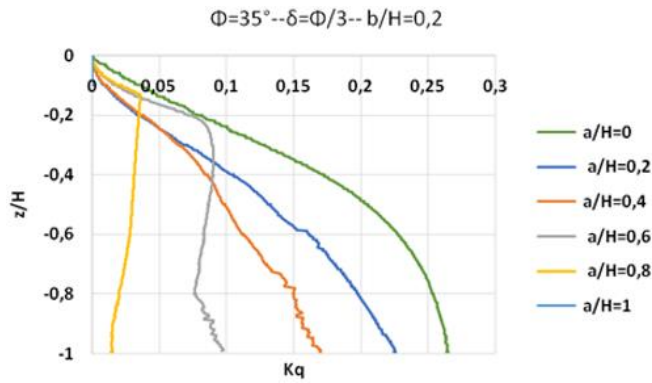


Figure 20. Pressure coefficient K_{aq} , $q/\gamma H=1$, $b/H=0.2$, $\Phi=35^\circ$, $\delta=\Phi/3$

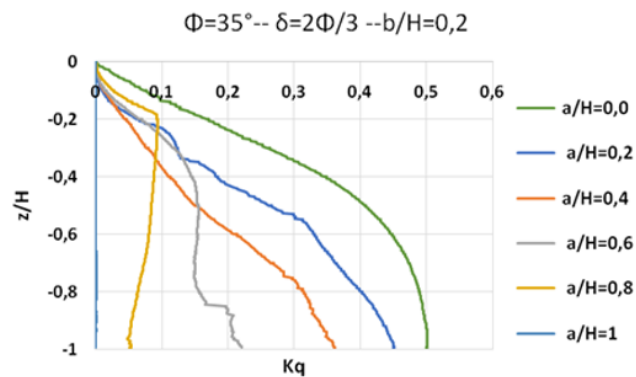


Figure 21. Pressure coefficient K_{aq} , $q/\gamma H=1$, $b/H=0.2$, $\Phi=35^\circ$, $\delta=2\Phi/3$

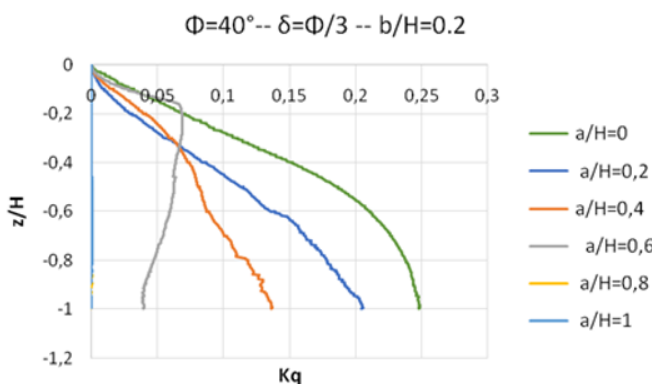


Figure 22. Pressure coefficient K_{aq} , $q/\gamma H=1$, $b/H=0.2$, $\Phi=40^\circ$, $\delta=\Phi/3$

In the case where the angle $\Phi=40^\circ$, (see Figures 22 and 23), from where the ratio $a/H=0.6$, z/H is limited to $z/H=-0.17$, and the maximum value of K_{aq} does not exceed $K_{aq}=0.06$ in the case where $\delta=\Phi/3$ and $K_{aq}=0.13$ in the case $\delta=2\Phi/3$, and from $a/H=0.8$ the value of K_{aq} takes the value $K_{aq}=0$.

(b) $q/\gamma H=1$, $b/H=0.3$

In the case where the angle $\Phi=30^\circ$ (Figures 24 and 25), one notices that the variation of the active coefficient pressure K_{aq} is linear up to a certain value, this value varies with the ratio a/H , then becomes constant, and the maximum value does not exceed $K_{aq}=0.35$ in the case where the position of the surcharge $a/H=0$ and $\delta=\Phi/3$ and $K_{aq}=0.70$ in the case where $\delta=2\Phi/3$, and one notices that the linear part becomes less important and the z/H ratio is limited to $z/H=-0.3$ from where the a/H ratio=0.8, and the maximum value of K_{aq} does not exceed $K_{aq}=0.1$ in the case where $\delta=\Phi/3$ and $K_{aq}=0.17$ in the case $\delta=2\Phi/3$ and from $a/H=1$, the value of K_{aq} takes the value $K_{aq}=0$.

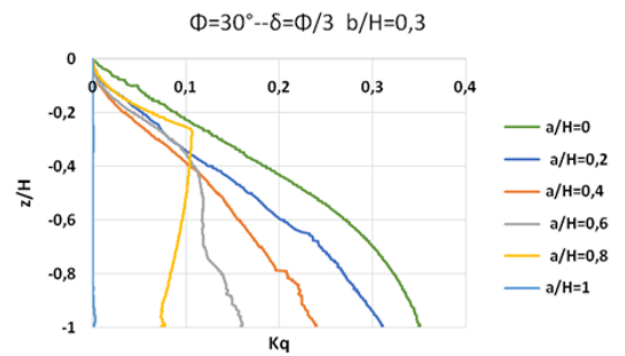


Figure 24. Pressure coefficient K_{aq} , $q/\gamma H=1$, $b/H=0.3$, $\Phi=30^\circ$, $\delta=\Phi/3$

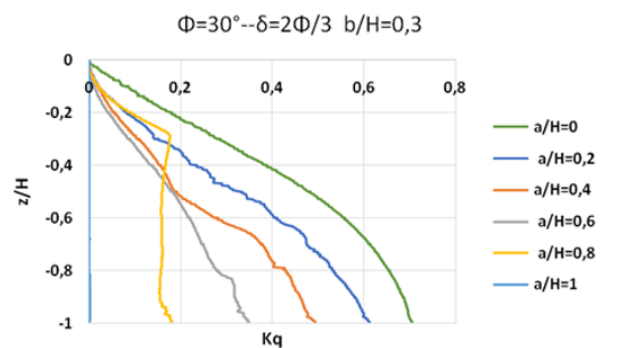


Figure 25. Pressure coefficient K_{aq} , $q/\gamma H=1$, $b/H=0.3$, $\Phi=30^\circ$, $\delta=2\Phi/3$

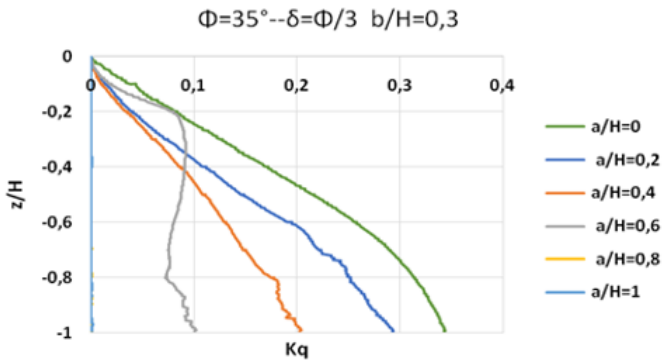


Figure 26. Pressure coefficient K_{aq} , $q/\gamma H=1$, $b/H=0.3$, $\Phi=35^\circ$, $\delta=\Phi/3$

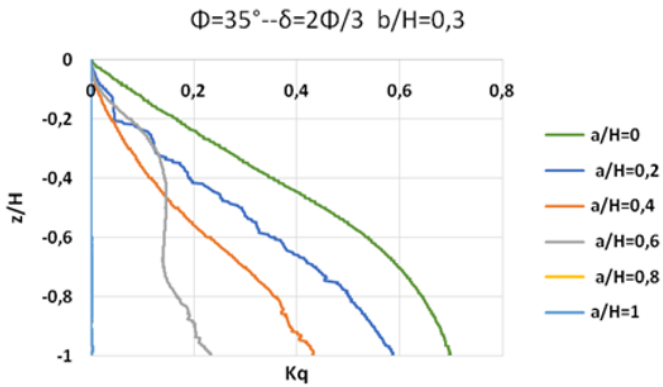


Figure 27. Pressure coefficient K_{aq} , $q/\gamma H=1$, $b/H=0.3$, $\Phi=35^\circ$, $\delta=2\Phi/3$

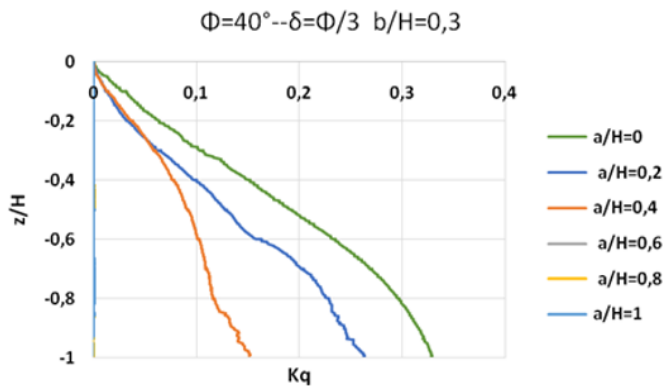


Figure 28. Pressure coefficient K_{aq} , $q/\gamma H=1$, $b/H=0.3$, $\Phi=40^\circ$, $\delta=\Phi/3$

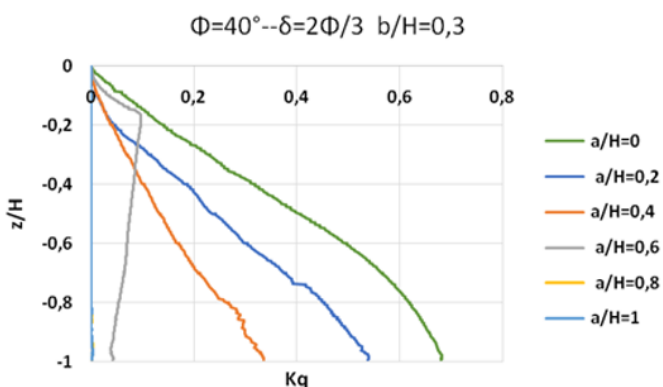


Figure 29. Pressure coefficient K_{aq} , $q/\gamma H=1$, $b/H=0.3$, $\Phi=40^\circ$, $\delta=2\Phi/3$

In the case where the angle $\Phi=35^\circ$ (Figures 26 and 27), one notices that the variation of active coefficient pressure K_{aq} is linear up to a certain value, this value varies with the ratio a/H , then becomes constant, and the maximum value does not exceed $K_{aq}=0.35$ in the case where the position of the surcharge $a/H=0$ and $\delta=\Phi/3$ and $K_{aq}=0.70$ in the case where $\delta=2\Phi/3$, and one notices that the linear part becomes less important and the z/H ratio is limited to $z/H=-0.2$ from where the a/H ratio=0.6, and the Max value of K_{aq} does not exceed $K_{aq}=0.08$ in the case where, $\delta=\Phi/3$ and $K_{aq}=0.1$ in the case $\delta=2\Phi/3$ and from $a/H=0.8$ the value of K_{aq} takes the value $K_{aq}=0$.

In the case where the angle $\Phi=40^\circ$ (Figures 28 and 29), one notices the same variation of active coefficient pressure K_{aq} as that of the other cases, and one notices that the linear part becomes less important and the report z/H is limited to $z/H=-0.17$ from where the ratio $a/H=0.6$, and the maximum value of K_{aq} does not exceed $K_{aq}=0.06$ in the case where $\delta=\Phi/3$ and from $a/H=0.6$ the value of K_{aq} takes the value $K_{aq}=0$, and $K_{aq}=0.13$ in the case $\delta=2\Phi/3$, and from $a/H=0.8$ the value of K_{aq} takes the value $K_{aq}=0$.

5.3 Failure mechanism

(a) $q/\gamma H=1$, $b/H=0.2$

A comparison of the shape of the potential failure planes, indicated by the concentrations of the plastic shear multiplier, shows that:

For the angle $\Phi=30^\circ$ (Figure 30), the failure plane tilt varies with the position of the surcharge a/H and the angle of friction δ has no influence on the shape of the fracture plane.

For the angle $\Phi=35^\circ$, the inclination of the failure plane varies with the position of the surcharge a/H , up to the value $a/H=0.8$ and from $a/H=0.9$, the surcharge has no influence on the failure plane and this latter merges with that of the case without surcharge.

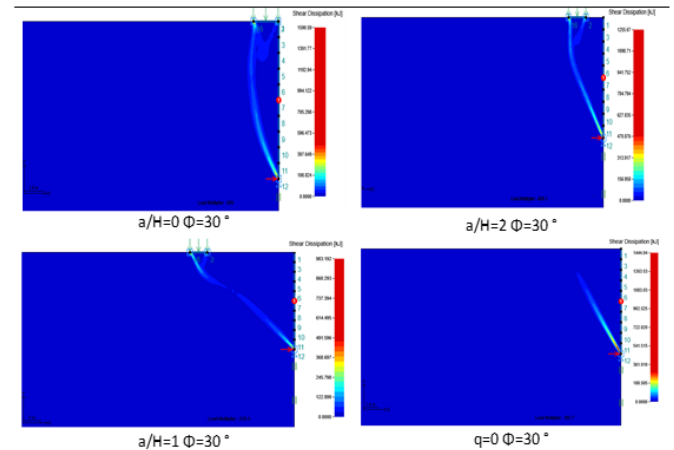


Figure 30. Collapse mechanism for retaining wall (upper bound) with intensity of plastic multiplier= 30°

For the angle $\Phi=40^\circ$, the inclination of the fracture plane varies with the position of the surcharge a/H , up to the value $a/H=0.6$ and from $a/H=0.7$, the surcharge has no influence on the failure plane and this latter merges with that of the case without surcharge.

(b) $q/\gamma H=1$, $b/H=0.3$

A comparison of the shape of the potential failure planes,

indicated by the concentrations of the plastic shear multiplier, shows that:

For the angle $\Phi=30^\circ$ (Figure 31), the failure plane tilt varies with the position of the surcharge a/H up to the value $a/H=0.9$ and from $a/H=1$, the surcharge has no influence on the failure plane and this latter merges with that of the case without surcharge.

For the angle $\Phi=35^\circ$, the inclination of the failure plane varies with the position of the surcharge a/H up to the value $a/H=0.7$ and from $a/H=0.8$, the surcharge has no influence on the failure plane and this latter merges with that of the case without surcharge.

For the angle $\Phi=40^\circ$, the inclination of the failure plane varies with the position of the surcharge a/H , up to the value $a/H=0.5$ and from $a/H=0.6$, the surcharge has no influence on the failure plane and this latter merges with that of the case without surcharge.

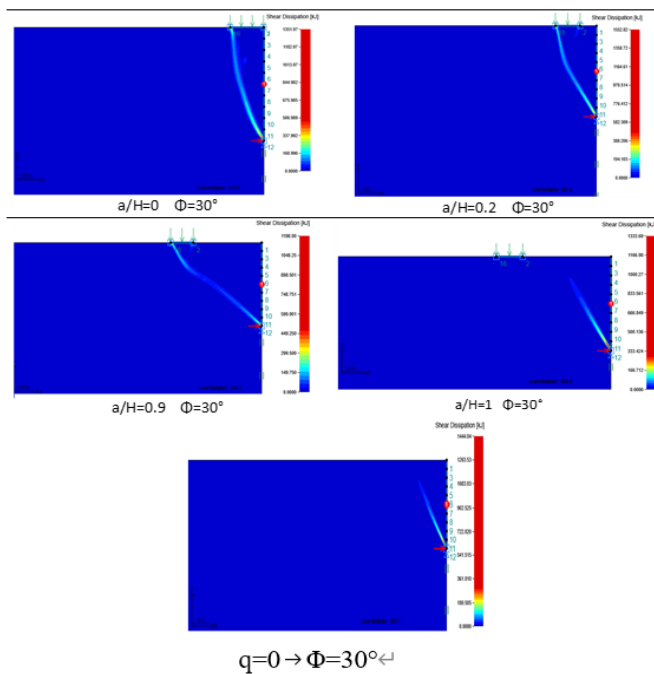


Figure 31. Collapse mechanism for retaining wall (upper bound) with intensity of plastic multiplier $\Phi=30^\circ$

6. CONCLUSIONS

A series of numerical calculations using the two-dimensional (2-D) EF limit analysis code OptumG2 [17] are performed in order to examine the effect of partial surcharge on the behavior of a retaining wall.

This study is based on the upper limit approach of the limit analysis for the evaluation of the earth's active pressure and the K_{aq} thrust coefficient when a uniformly distributed partial surcharge acts on the backfill.

The analysis evaluates the active earth lateral pressure with various uniformly distributed partial surcharge conditions and soil properties.

The comparison of the present analysis with the conventional Coulomb method proposed by Steinfeldt and Hansen [14], Motta [15] and Greco [16] as well as with the method presented by Ghanbari and Taheri [24], indicates good compatibility.

The results are presented as dimensionless graphs. The main

conclusions based on these results can be outlined as follows:

The effect of the surcharge on the lateral pressure and on the active thrust coefficient depends on the position of the load, the width of the surcharge and the internal friction angle of the soil; for the rupture mechanism, one notes that the plane of failure depends on the angle of internal friction of the soil of the ratio a/H and that the angle of friction between the Backfill and the wall δ has no influence on the shape of the plane of breaking up.

In the case where the load intensity $q/\gamma H=1$ and the ratio of the width of the load b to the height H of the retaining wall $b/H=0.2$, if the internal friction angle of the soil $\Phi=30^\circ$ we note that the variation of the lateral pressure is almost linear for the values of the ratio $a/H=0, 0.2$ and 0.4 ; from $a/H=0.6$, we distinguish two parts, one increasing until the ratio $z/H=-0.3$ then changes slope with a smaller variation, and the importance of the pressure decreases with the increase in the a/H ratio, and the lateral pressure increases with the increase in the friction angle δ , for the angle $\Phi=35^\circ$, the effect of the surcharge becomes zero when $a/H=1$, if the angle $\Phi=40^\circ$, the effect of the surcharge becomes zero from $a/H=0.8$.

Regarding the effect of the surcharge on the active thrust coefficient, we notice that the value of the K_{aq} thrust coefficient increases at the beginning up to a limit value, this value varies with the variation of the a/H ratio, then stabilizes, and its value is maximum in the case where the position of the surcharge $a/H=0$, from where the ratio $a/H=1$ for $\Phi=30^\circ$ and $a/H=0.8$. For $\Phi=35^\circ$, the thrust coefficient takes the value $K_{aq}=0$.

A comparison of the shape of the potential failure planes, indicated by the concentrations of the plastic shear multiplier, for the angle $\Phi=30^\circ$, the failure plane tilt varies with the position of the surcharge a/H and the surcharge has no influence on the shape of the fracture plane.

A comparison of the shape of the potential failure planes, indicated by the concentrations of the plastic shear multiplier, shows that:

For the angle $\Phi=30^\circ$, the failure plane tilt varies with the position of the surcharge a/H and the angle of friction δ has no influence on the failure plane.

In the case of the ratio $b/H=0.3$, for the angle $\Phi=30^\circ$ and from $a/H=0.8$, we distinguish two parts: one increasing until the ratio $z/H=-0.28$ then changes slope with a smaller variation, and the effect of the surcharge becomes zero from $a/H=1$, if the angle $\Phi=35^\circ$, the effect of the surcharge becomes zero from $a/H=0.8$ and if the angle $\Phi=40^\circ$, the effect of the surcharge becomes zero from $a/H=0.6$. For the effect of the surcharge on the active pressure coefficient, from where the ratio $a/H=1$ for $\Phi=30^\circ$ and $a/H=0.8$ for $\Phi=35^\circ$ and $\Phi=40^\circ$ the value of K_{aq} remains equal to zero.

Finally, we note that the effect of the surcharge decreases with the increase in the width of the surcharge and the increase in the friction angle of the backfill.

REFERENCES

- [1] Coulomb C.A. (1776). Essai sur une application des règles de maximis & minimis à quelques problèmes de statique, relatifs à l'architecture. Mémoires de Mathématiques et de Physique Présentés à l'Académie Royale des Sciences par Divers Savants, et Lus sans ses Assemblées, 7: 343-382.

- [2] Rankine, W.J.M. (1857). II. On the stability of loose earth. *Philosophical transactions of the Royal Society of London*, (147): 9-27.
- [3] Kumar, J., Chitikela, S. (2002). Seismic passive earth pressure coefficients using the method of characteristics. *Canadian Geotechnical Journal*, 39(2): 463-471. <https://doi.org/10.1139/t01-103>
- [4] Santhoshkumar, G., Ghosh, P. (2018). Seismic passive earth pressure on an inclined cantilever retaining wall using method of stress characteristics—A new approach. *Soil Dynamics and Earthquake Engineering*, 107: 77-82. <https://doi.org/10.1016/j.soildyn.2018.01.021>
- [5] Muraro, S., Madaschi, A., Gajo, A. (2015). Passive soil pressure on sloping ground and design of retaining structures for slope stabilisation. *Géotechnique*, 65(6): 507-516. <https://doi.org/10.1680/geot.14.P.211>
- [6] Chowdhury, S.S. (2019). A study on lateral earth pressure against strutted retaining wall in cohesionless soil deposit. *International Journal of Geotechnical Engineering*, 13(2): 122-138. <https://doi.org/10.1080/19386362.2017.1326683>
- [7] Veiskarami, M., Jamshidi Chenari, R., Jameei, A.A. (2019). A study on the static and seismic earth pressure problems in anisotropic granular media. *Geotechnical and Geological Engineering*, 37(3): 1987-2005. <https://doi.org/10.1007/s10706-018-0739-9>
- [8] Krey, H. (1936). *Erddrucke, Erdwiderstand und Tragfähigkeit des Baugrundes*. W. Ernst und Sohn, Berlin, 5e ed.
- [9] Caquot, A., Kerisel, J. (1956). *Traité de Mécanique des sols*, 3. GauthierVillars Editeurs, Paris, 558 p.
- [10] Gaudin, C., Riou, Y., Popa, H., Garnier, J. (2002). Numerical modelling of centrifuge test on embedded wall. In *Numerical modelling of centrifuge test on embedded wall*, Paris, France, pp. 1-7.
- [11] Blum, H. (1951). Beitrag zur Berechnung von Bohlwerken: unter Berücksichtigung der Wandverformung, insbesondere bei mit der Tiefe linear zunehmender Widerstandsziffer. Ernst & Sohn.
- [12] Jarquio, R. (1981). Total lateral surcharge pressure due to strip load. *Journal of the Geotechnical Engineering Division*, 107(10): 1424-1428.
- [13] Misra, B. (1980). Lateral pressures on retaining walls due to loads on surface of granular backfill. *Soils and Foundations*, 20(2): 31-44. https://doi.org/10.3208/sandf1972.20.2_31
- [14] Steenfelt, J.S., Hansen, B. (1983). Discussion to "Total Lateral Surcharge Pressure Due to Strip Load" by Ramon Jarquio (October, 1981). *Journal of Geotechnical Engineering*, 109(2): 271-273.
- [15] Motta, E. (1994). Generalized Coulomb active-earth pressure for distanced surcharge. *Journal of Geotechnical Engineering*, 120(6): 1072-1079.
- [16] Greco, V.R. (2006). Lateral earth pressure due to backfill subject to a strip of surcharge. *Geotechnical & Geological Engineering*, 24(3): 615-636. <https://doi.org/10.1007/s10706-005-2009-x>
- [17] Krabbenhoft, K., Lyamin, A., Krabbenhoft, J. (2015). *Optum computational engineering (OptumG2)*. Computer Software.
- [18] Georgiadis, M., Anagnostopoulos, C. (1998). Lateral pressure on sheet pile walls due to strip load. *Journal of Geotechnical and Geoenvironmental Engineering*, 124(1): 95-98. [https://doi.org/10.1061/\(ASCE\)1090-0241\(1998\)124:1\(95\)](https://doi.org/10.1061/(ASCE)1090-0241(1998)124:1(95))
- [19] Caltabiano, S., Cascone, E., Maugeri, M. (2012). Static and seismic limit equilibrium analysis of sliding retaining walls under different surcharge conditions. *Soil Dynamics and Earthquake Engineering*, 37: 38-55. <https://doi.org/10.1016/j.soildyn.2012.01.015>
- [20] Singh, A.P., Chatterjee, K. (2020). Ground settlement and deflection response of cantilever sheet pile wall subjected to surcharge loading. *Indian Geotechnical Journal*, 50(4): 540-549. <https://doi.org/10.1007/s40098-019-00387-1>
- [21] Singh, A.P., Chatterjee, K. (2020). Influence of soil type on static response of cantilever sheet pile walls under surcharge loading: A numerical study. *Arabian Journal of Geosciences*, 13(3): 1-11. <https://doi.org/10.1007/s12517-020-5170-x>
- [22] Farzaneh, O., Askari, F., Fatemi, J. (2014). Active earth pressure induced by strip loads on a backfill. *International Journal of Civil Engineering*, 12(4): 281-291.
- [23] Hou, G., Shu, S. (2019). Trial wedge approach to determine lateral earth pressures. *International Journal of Geomechanics*, 19(1): 06018035. [http://dx.doi.org/10.1061/\(ASCE\)GM.1943-5622.0001326](http://dx.doi.org/10.1061/(ASCE)GM.1943-5622.0001326)
- [24] Ghanbari, A., Taheri, M. (2012). An analytical method for calculating active earth pressure in reinforced retaining walls subject to a line surcharge. *Geotextiles and Geomembranes*, 34: 1-10. <https://doi.org/10.1016/j.geotexmem.2012.02.009>
- [25] Chauhan, V.B., Dasaka, S.M. (2021). Behavior of rigid retaining walls with relief shelves: An analytical approach. *Geotechnical and Geological Engineering*, 40: 663-675. <https://doi.org/10.1007/s10706-021-01913-w>